archives
of thermodynamics
Vol. **43**(2022), No. 1, 21–43
DOI: 10.24425/ather.2022.140923

Implementation of turbulence damping in the OpenFOAM multiphase flow solver interFoam

JIRI POLANSKY[a*]
SONJA SCHMELTER[b]

[a] Czech Technical University in Prague, Jugoslávských partyzánů 1580/3, 160 00 Prague 6 – Dejvice, Czech Republic

[b] Physikalisch-Technische Bundesanstalt (PTB), Abbestraße 2-12, D-10587 Berlin-Charlottenburg, Germany

Abstract In the presented work Egorov's approach (adding a source term to the ω-equation in the k-ω model, which mimics the damping of turbulence close to a solid wall) was implemented in on the subclass of shear stress transport models. Hence, turbulence damping is available for all shear stress transport type models, including hybrid models that are based on the ω-equation. It is shown that turbulence damping improves the prediction of the axial velocity profile not only for Reynolds-averaged Navier–Stokes simulation but also for detached eddy simulation and delayed detached eddy simulation models. Furthermore, it leads to a more realistic estimation of the pressure drop and, hence, to a more correct prediction of the liquid level. In this paper, simulation results for four different turbulence models are presented and validated by comparison with experimental data. Furthermore, the influence of the magnitude of the damping factor on the pressure drop in the channel is investigated for a variety of different gas-to-liquid flow rate ratios. These investigations show that higher gas-to-liquid flow rate ratios require higher damping factors to correctly predict the pressure drop. In the end, advice is formulated on how an appropriate damping factor can be determined for a specific test case.

Keywords: Multiphase flow; Stratified flow; Turbulence damping; Computational fluid dynamics; OpenFOAM; Reynolds-averaged Navier–Stokes; Detached eddy simulation; Delayed detached eddy simulation

*Corresponding Author. Email: jiri.polansky@cvut.cz

Nomenclature

A	–	interfacial area density
a_1	–	turbulence model closure coefficient
B	–	damping factor
C_{DES}	–	constant in DES turbulence model
$C_{d1},\ C_{d2}$	–	constants in DES turbulence model
D_{hydr}	–	hydraulic diameter
$F_1,\ F_2$	–	blending functions in turbulence model
f_d	–	delay function
H	–	height of the channel, m
k	–	turbulent kinetic energy, J
L	–	length of the channel, m
l	–	length scale in turbulence model, m
p	–	static pressure, Pa
Re	–	Reynolds number
r_d	–	parameter in DDES model
S	–	magnitude of strain rate, Hz
S_ω	–	source term in ω-equation, Hz
$U = (U_1, U_2, U_3)^{\mathrm{T}}$	–	mean velocity, m/s
W	–	width of the channel, m
X	–	flow quality
$x = (x_1, x_2, x_3)^{\mathrm{T}}$	–	spatial (Cartesian) coordinate, m
y	–	distance to the nearest wall, m

Greek symbols

α	–	volume fraction
β	–	turbulence model closure coefficient
β^*	–	turbulence model closure coefficient
δn	–	cell height normal to interface
Δ	–	largest dimension of local grid cell
κ	–	von Karman constant
λ	–	friction factor
μ	–	dynamic viscosity, kg m/s
ν	–	kinematic viscosity, m^2 s
ν_t	–	turbulent viscosity, m^2/s
Ω	–	magnitude of vorticity tensor, Hz
ω	–	specific dissipation rate, Hz
ρ	–	density, kg/m^3
$\sigma_{\omega 2}$	–	turbulence model closure coefficient
ε	–	dissipation rate of turbulent kinetic energy, $\mathrm{m}^2/\mathrm{s}^2$

1 Introduction

Free surface flow is one of the most important multiphase flow regimes primarily because of its presence in extensive industrial applications, such as oil transportation, steam generators, evaporators, condensers, and boiling

water reactors. There is a great need to have specific techniques capable of extracting characteristics of free surface flow pattern *via* experiment and numerical modelling. An important issue in modelling gas-liquid flows is the treatment of turbulence at the interface between the two phases. In industrial applications, turbulence is often modelled using a Reynolds-averaged Navier–Stokes approach. It is well known that, for this method, turbulent viscosity is overpredicted in the vicinity of the interface. To overcome this problem, Egorov *et al.* [1] proposed to add a source term to the ω-equation in the k-ω model, which mimics the damping of turbulence close to a solid wall.

Stratified two-phase flow regimes occur in a variety of applications, for example in main cooling lines of pressurized water reactors, chemical plants, or oil pipelines [3]. In many of these applications, it is important to avoid the occurrence of slugs because they are leading to safety issues. Hence, it is crucial for an appropriate computational fluid dynamics (CFD) model to correctly predict the generation of waves and slugs in stratified flows. To achieve this, the interfacial momentum exchange and turbulence parameters need to be modelled correctly [4].

For a wide range of engineering applications, turbulence is modelled by the Reynolds-averaged Navier–Stokes (RANS) approach together with a turbulent viscosity formulation. It is well-known that, without any special treatment of the free surface, the high-velocity gradients near the interface generate turbulence at levels that are physically impossible, in particular in different eddy-viscosity models like k-ε or k-ω models [4,5]. Therefore, damping of turbulence is necessary in the vicinity of the interface between the phases. Egorov *et al.* [1] proposed a damping procedure, which has later been implemented in several CFD codes. The idea of this approach is that, at the interface between two phases, the lighter (gas) phase may see the heavier (liquid) phase like a solid wall, suggesting a wall-like treatment of turbulent dissipation at the interface [5]. Egorov *et al.* [1] modelled this by introducing a source term in the ω-equation of the k-ω model, which becomes only active near the gas-liquid interface. This approach was implemented by means of a user-defined function in commercial software Ansys CFX-5, see [1] for details.

Later, many authors followed Egorov's idea and implemented turbulence damping in the commercial general purpose computational fluid dynamic code Ansys CFX, see, e.g., [3,6–8]. Furthermore, Egorov's approach is also available in commercial Ansys Fluent software for modeling fluid flow, heat transfer, turbulence and reactions for industrial applications, see [9]. In [10],

it was used to simulate stratified air-water flow. The authors compared simulation results with and without turbulence damping and concluded that the employment of Egorov's source term improved the prediction of the pressure drop and of the hold-up.

In [11], turbulence damping was used as part of the large scale interface (LSI) model implemented in the commercial multiphysics computational fluid dynamics (CFD) software STAR-CCM+. Comparison with experimental data from Fabre *et al.* [2] showed a significant improvement of the axial velocity profile for the case that damping is applied. Furthermore, damping enhances the prediction of the correct pressure losses. The latter one was already observed by Lo and Tomasello [12] who applied Egorov's turbulence damping approach in the preceding software STAR-CD package.

To the authors' knowledge, Frederix *et al.* [5] were the first who implemented Egorov's turbulence damping approach in the open-source multiphysics software package OpenFOAM. Besides the 'classical' implementation within the k-ω model, they also extended the approach to the k-ε model. They validated their results by comparison with experimental data from Fabre *et al.* [2]. Later, Fan *et al.* [13] used Egorov's turbulence damping approach within the k-ω shear stress transport (SST) model for the simulation of annular flow with disturbance waves. In [14], a new length scale for Egorov's model was introduced to overcome the dependency of the damping factor on the refinement level of the mesh used for the simulation. Furthermore, an asymmetric treatment for the damping terms was proposed. These extensions and enhancements are all included in varRhoTurbVOF2, a set of OpenFOAM volume of fluid (VOF) solvers for turbulent isothermal multiphase flows, which are variable-density incompressible, see [15].

In the presented work, Egorov's turbulence damping approach was implemented for OpenFOAM's multiphase flow solvers. The source term was added to the right-hand side of the ω-equation into kOmega.C and kOmega SST.C files. Therefore, the modification is available for all turbulence models that are either based on the k-ω or on the k-ω SST model, namely: the (standard) k-ω model [16], the k-ω SST model [17], the four-equation transitional Langtry-Menter k-ω SST model [18], the k-ω SST scale-adaptive simulation (SAS) model [19], the k-ω SST detached eddy simulation (DES) model [20], and the k-ω SST (improved) delayed detached eddy simulation (DDES and IDDES) model [21]. The implementation was validated by means of the well-known co-current air-water channel flow described in Fabre *et al.* [2]. Not only the axial velocity profiles, pressure drop and

turbulence parameters were compared as in [5, 14], but also the height of the liquid level as well as the axial velocity in the whole cross-section. The latter one gives insight into how the different turbulence models perform and where there are their advantages and disadvantages.

In this paper, the results of four different turbulence models are compared with each other as well as with corresponding experimental data from Fabre *et al.* [2], namely:

1) the standard k-ω model [16] (abbreviated by k-ω in the following),
2) the 2003 version of the k-ω SST model [17] (abbreviated by SST in the following),
3) the k-ω SST DDES model [21] (abbreviated by DDES in the following), and
4) the k-ω SST DES model [20] (abbreviated by DES in the following).

This comparison investigates not only the performance of turbulence damping in RANS models as in [5, 14], but also for DDES and DES.

Furthermore, the choice of the magnitude of the damping factor is investigated in this work. Previously, Chinello *et al.* [10] showed that a damping factor of 250 was sufficient for their application and that a further increase did not affect the results anymore. However, for the cases considered in this paper, higher damping factors are needed. This shows that the choice of the damping factor depends on the considered application. In order to give advice on how to choose an appropriate damping factor in general, a systematic study for eleven different gas-to-liquid flow rate ratios and six different damping factors has been performed.

2 Simulation set-up and implementation of turbulence damping

2.1 Geometry and boundary conditions

In this paper, we consider the co-current flow of water and air through a channel of length $L = 16$ m, height $H = 0.1$ m, and width $W = 0.2$ m. In Fig. 1, the considered set-up is drawn schematically. The fluid properties of both phases, air and water are summarized in Table 1.

For the numerical simulation, we choose the flow conditions according to the experimental set-up in Fabre *et al.* [2] leading to a volume flow rate

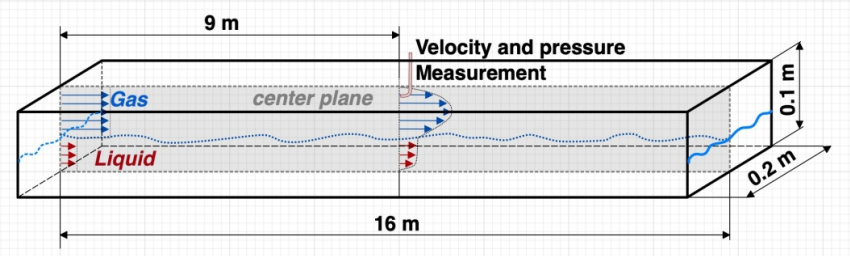

Figure 1: Schematic drawing of the considered geometry.

Table 1: Material and transport properties.

Parameter	Value	Unit
Water density	1000	kg/m^3
Air density	1	kg/m^3
Water kinematic viscosity	1.00×10^{-6}	m/s^2
Air kinematic viscosity	1.48×10^{-5}	m/s^2
Surface tension of water in air	0.07	N/m
Contact angle of water on smooth surface	72	deg

of 3 l/s for water and 45.4 l/s for air. Table 2 presents some parameters of interest, such as superficial velocity, Reynolds and Froude number, which can be derived from the flow rates. Note that the Reynolds number has been calculated based on the superficial velocity, whereas for the calculation of the Froude number the average flow velocity (averaged over the cross-section perpendicular to the flow direction) has been used.

Table 2: Flow conditions.

Parameter	Water	Air	Unit
Superficial velocity	0.15	2.27	m/s
Reynolds number	1.65×10^4	1.45×10^4	–
Froude number	0.6465	–	–

Additional simulations for a variety of different gas volume flow rates have been performed to investigate the influence of the magnitude of the damping factor on the resulting pressure drop in the channel. For this, test cases with the following gas flow rates have been considered: 15, 25, 35, 45.4, 55, 65, 75.4, 85, 95, 105, and 118.7 l/s.

For the numerical solution of this multiphase flow problem, the OpenFOAM solver interFoam is used. InterFoam is a solver for two incompressible, isothermal, and immiscible fluids based on the volume of fluid method. For this, the computational domain was discretized into 3 932 160 hexahedral cells, using blockMesh utility. For a realistic simulation, the inlet was split up into two parts and a separate air and water inlet was defined. The height of liquid at the inlet corresponds to the level of water known from the corresponding experiment. Since a simple wavy multiphase flow pattern is expected, the outlet for the velocity and void fraction are defined as zero gradient boundary conditions. The list of boundary conditions on inlet and outlet parts is presented in Table 3. The turbulent flow close to the wall is simulated with wall functions. Two different approaches were tested, namely high and low Reynolds number conditions, see Table 4. Both approaches led to the same results at the considered output plane ($x_3 = 9$ m). Thus, all presented results have been derived using the high Reynolds number boundary conditions.

Table 3: Inlet and outlet boundary conditions.

Variable	Air inlet	Water inlet	Outlet
Velocity	flow Rate Inlet Velocity	flow Rate Inlet Velocity	zero Gradient
Void fraction	inlet Outlet	inlet Outlet	zero Gradient
Pressure	fixed Flux Pressure	fixed Flux Pressure	fixed Value

Table 4: Turbulent parameters, wall boundary conditions.

Variable	High Re		Low Re	
	Type	Value	Type	Value
k	kqRWallFunction	1	fixedValue	10–12
ω	omegaWallFunction	1	omegaWallFunction	10^9
ν_t	nutkWallFunction	0	nutUSpaldingWallFunction	0

2.2 Turbulence model description

In the following, the basic ideas of the different turbulence models that have been used in this paper are briefly introduced.

2.2.1 Implementation of the k-ω SST model in OpenFOAM

The SST model is a mix between the k-ε model [23] and the k-ω model [16]. The idea is to blend between these two standard models in such a way that each model is applied in the region, where it performs best. Thus, the k-ω model is used in the vicinity of the walls, whereas the k-ε model is applied in the freestream regions.

In the OpenFOAM solver, the variant of the k-ω SST model by Menter *et al.* [17] is implemented. As in the original version of the k-ω SST model, see [24], the switch between k-ε and k-ω model is realized by means of the following blending function:

$$F_1 = \tanh\left(\Phi^4\right), \qquad \Phi = \min\left[\max\left(\frac{\sqrt{k}}{\beta^*\omega y}, \frac{500\nu}{y^2\omega}\right), \frac{4\rho\sigma_{\omega 2}k}{CD_{k\omega}y^2}\right] \tag{1}$$

with $CD_{k\omega} = \max\left(2\rho\sigma_{\omega 2}\frac{1}{\omega}\frac{\partial k}{\partial x_i}\frac{\partial \omega}{\partial x_i}, 10^{-10}\right)$, $\beta^* = 0.09$, and $\sigma_{\omega 2} = 0.856$, where y denotes the distance to the nearest wall. F_1 is zero away from the surface (k-ε model) and becomes one inside the boundary layer (k-ω model).

The turbulent eddy viscosity is defined as follows:

$$\nu_t = \frac{a_1 k}{\max\left(a_1\omega, SF_2\right)}, \tag{2}$$

where S is the invariant measure of the strain rate, $a_1 = 0.31$, and F_2 is a second blending function, defined as

$$F_2 = \tanh\left(\Psi^2\right), \qquad \Psi = \max\left(\frac{2\sqrt{k}}{\beta^*\omega y}, \frac{500\nu}{y^2\omega}\right). \tag{3}$$

Furthermore, the SST model uses a limiter for the production term

$$P_k = \nu_t\rho\frac{\partial U_i}{\partial x_j}\left(\frac{\partial U_i}{\partial x_j} + \frac{\partial U_j}{\partial x_i}\right)$$

to prevent the build-up of turbulence in the stagnation regions:

$$P_k \longrightarrow \widetilde{P^k} = \min(P_k, 10\,\beta^*\rho k\omega). \tag{4}$$

2.2.2 Implementation of SST–DES and SST–DDES in OpenFOAM

The idea of DES and DDES hybrid models is to combine the RANS technology in the boundary layers (where large eddy simulation (LES) would be too costly) with an LES in the separated regions. In this approach, a one equation turbulence model is used, which functions as a subgrid-scale model in the regions, where the grid is fine enough for an LES, and as a RANS model in regions, where it is not [20]. In OpenFOAM toolbox several DES and DDES models are available.

To transform the k-ω SST model into DES mode, the dissipative term of the k-equation is modified as follows:

$$D^k_{\mathrm{RANS}} = \rho\beta^* k\omega = \rho k^{3/2}/l_{\mathrm{RANS}} \quad \longrightarrow \quad D^k_{\mathrm{DES}} = \rho k^{3/2}/l_{\mathrm{DES}}\,, \tag{5}$$

where $l_{\mathrm{RANS}} = k^{1/2}/(\beta^*\omega)$ is the length scale of the underlying RANS model and l_{DES} denotes the DES length scale. It is given by

$$l_{\mathrm{DES}} = \min\left(l_{\mathrm{RANS}},\ C_{\mathrm{DES}}\Delta\right), \tag{6}$$

where Δ is the largest dimension of the local grid cell and C_{DES} is an adjustable model constant. In [20], this constant has been calibrated for the two branches of the k-ω SST model separately:

$$C_{\mathrm{DES}} = (1 - F_1)\, C^{k-\varepsilon}_{\mathrm{DES}} + F_1 C^{k-\omega}_{\mathrm{DES}}\,. \tag{7}$$

Here, F_1 is the blending function of the k-ω SST model, see Eq. (1). In OpenFOAM, the following values are used: $C^{k-\varepsilon}_{\mathrm{DES}} = 0.6$ and $C^{k-\omega}_{\mathrm{DES}} = 0.82$.

In regions, where the grid is fine enough in all directions, the term $C_{\mathrm{DES}}\Delta$ becomes smaller than the length scale of the underlying RANS model l_{RANS}. This reduces k, which leads to a decrease of the turbulent viscosity. Thus, in regions, where the mesh is fine enough to resolve turbulence, the model reduces the amount of modelled turbulent shear stress and allows the region to be treated with LES. A well-known problem with this formulation occurs in near-wall regions. Since the grid close to the walls is often very fine, it can happen that the solution is triggered to go unsteady here. However, this is generally an unrealistic result since the turbulent structures near the wall are very small and require an extremely fine grid to be resolved properly with LES. These requirements might not be satisfied by the mesh and, hence, a poorly resolved LES close to the walls might be the result.

Therefore, the DDES model introduces an additional term, which allows to "refuse" the switch to LES mode in case the point is well inside a boundary layer, see [25]. The SST–DDES model, see [21], combines the SST–DES formulation of Strelets [20] with the DDES shielding functions of Spalart *et al.* [25]. In this model, the length scale l_{DES} of the DES approach, see Eq. (6), is substituted by l_{DDES} defined as follows:

$$l_{\mathrm{DDES}} = l_{\mathrm{RANS}} - f_d \max\left(0,\ l_{\mathrm{RANS}} - l_{\mathrm{LES}}\right). \tag{8}$$

Here $l_{\mathrm{RANS}} = k^{1/2}/(\beta^*\omega)$ and $l_{\mathrm{LES}} = C_{\mathrm{DES}}\Delta$, where C_{DES} is given by Eq. (7). The delay function f_d is defined as

$$f_d = 1 - \tanh\left[(C_{d1} r_d)^{C_{d2}}\right] \quad r_d = \frac{\nu_t + \nu}{\kappa^2 y^2 \sqrt{\frac{1}{2}\left(S^2 + \Omega^2\right)}}, \tag{9}$$

where $C_{d1} = 20$ and $C_{d2} = 3$. Furthermore, $\kappa = 0.41$ is the von Karman constant, y denotes the distance to the wall, and S and Ω are the magnitudes of the strain rate and vorticity tensor, respectively.

2.3 Implementation of turbulence damping

In free surface flows, a high velocity gradient at the interface between two fluids results in the generation of high turbulence in both phases. Therefore, turbulence damping in the interfacial region is necessary for correct modelling of multiphase flows.

The present study focuses on the implementation of turbulence damping in models that are based on the ω-equation. The following term, originally proposed by Egorov *et al.* [1], is added as an additional source term to the right-hand side of the ω-equation for each phase i:

$$S_{\omega,i} = A\Delta n \beta \rho_i \left(B \frac{6\mu_i}{\beta \rho_i \Delta n^2}\right)^2. \tag{10}$$

Here, A is the interfacial area density given by

$$A = |\nabla \alpha_i| \, \Delta n, \tag{11}$$

where α_i is the volume fraction of phase i. For two-phase flow, it holds $\alpha_1 = 1 - \alpha_2$, and hence $|\nabla \alpha_1| = |\nabla \alpha_2|$. Furthermore, Δn is the typical grid cell size across the interface, $\beta = 0.075$, and ρ_i and μ_i are the density and viscosity of phase i. B is a model parameter, which has to be adapted, in [1], a value of 100 is proposed.

The parameter Δn is calculated based on grid information. In this paper, two different approaches are used. In the first one, which is sufficient for stratified or wavy flow, simply the size of the cells perpendicular to the main flow direction (defined by the user) is used. In the second, more general approach, the size of the cells corresponding to the maximal gradient of the volume fraction are used. This approach is also feasible for flow patterns, where the direction of the interface cannot be assumed to be mainly horizontal but changes from horizontal to vertical, e.g. for slug flow. Figure 2 illustrates this. For each cell, the maximum gradient of the volume fraction α is calculated and the size of the cell in the corresponding direction (Δx_1, Δx_2 or Δx_3) is used as a value for Δn.

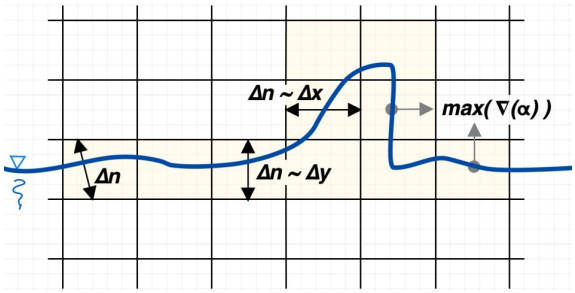

Figure 2: Illustration of the approximation of Δn for different orientations of the gas-liquid interface.

3 Results

In this section, simulation results of the test case described in the previous section are presented. This test case has been simulated with four different turbulence models, which have been improved by turbulence damping. In the following, the results for the different turbulence models will be compared with each other. Furthermore, the influence of turbulence damping on the different models and parameters will be discussed. In the end, the influence of the magnitude of the damping factor on the resulting pressure drop in the channel will be investigated for a variety of different gas flow rates.

3.1 Effect of damping on turbulence parameters

Figure 3 shows profiles of the specific rate of dissipation, ω, for four different turbulence models (k-ω, SST, DDES, and DES). In each picture, the profiles

are plotted for four different damping factors: $B = 0$, 1000, 3000, and 6000. Considering the profiles obtained with the different turbulence models without turbulence damping ($B = 0$), one observes that the k-ω model does not recognize the interface between the two phases. In contrast, the other models show an increase of ω close to the interface also for $B = 0$. Let us now consider the effect of turbulence damping on the ω-profiles. For all turbulence models, one observes a strong increase of ωclose to the interface with increasing values of B. This can directly be explained by Eqs. (10) and (11): At the interface, A becomes larger than zero and, hence, leads to $S_{\omega,i} > 0$. Since $S_{\omega,i}$ is an additional source term in the ω-equation, this leads to an increase of ω.

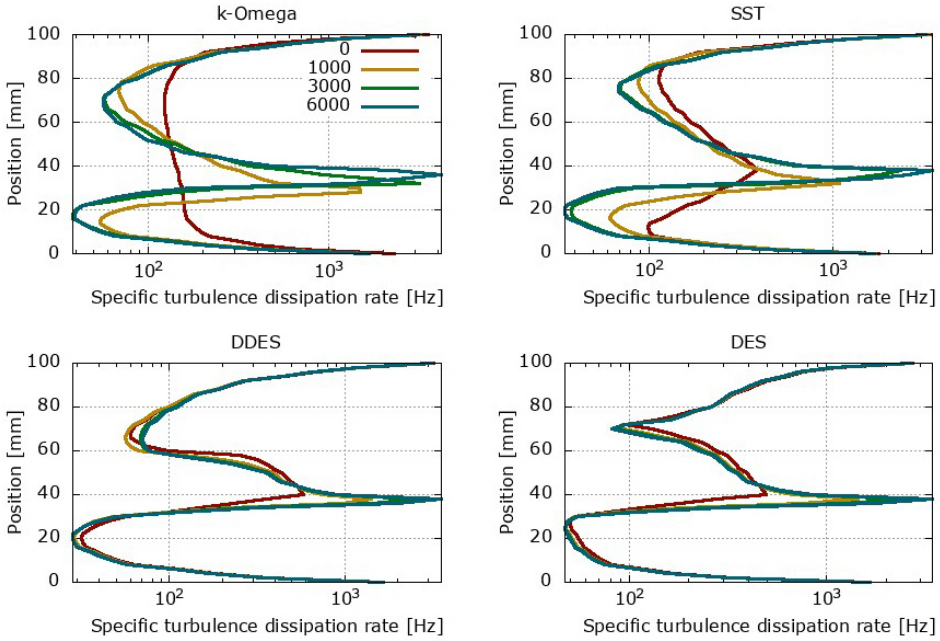

Figure 3: Profiles of the specific rate of dissipation, ω, in the centre plane at $x_3 = 9$ m (see Fig. 1) for four different turbulence models (top left – standard k-ω model, top right – k-ω SST model, bottom left – hybrid SST–DDES model, bottom right – hybrid SST–DES model) and four different damping factors ($B = 0$, 1000, 3000, and 6000).

As described previously, the idea of turbulence damping is that the lighter gas phase sees the interface like a wall. Thus, an increase of ω to similar values as close to the walls is the desired effect of turbulence damping. For all turbulence models, this effect is obtained for $B = 3000$ and 6000. For

the hybrid models (DDES and DES), the desired increase is already visible for $B = 1000$.

Figure 4 shows profiles for the turbulent viscosity, ν_t, for the same turbulence models and values of B as considered in Fig. 3. They show a similar, but inverse behaviour as the ω-profiles: While turbulence damping leads to an increase of ω at the interface, the turbulent viscosity decreases in this region. As previously observed for ω, the liquid-gas interface is not recognized by the standard k-ω model without turbulence damping ($B = 0$). Also for the SST and the DES model, only a very low decrease of ν_t at the interface can be observed without damping. Regarding ν_t, the DDES model seems to perform best of the four considered turbulence models for $B = 0$.

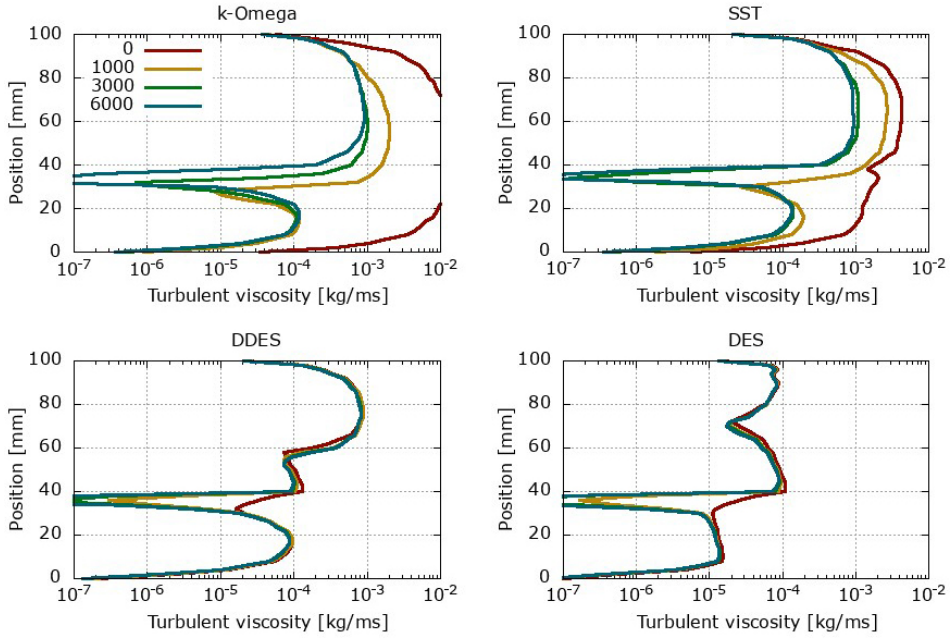

Figure 4: Profiles of the turbulent viscosity, ν_t, in the centre plane at $x_3 = 9$ m (see Fig. 1) for four different turbulence models (top left – standard k-ω model, top right – k-ω SST model, bottom left – hybrid SST–DDES model, bottom right – hybrid SST–DES model) and four different damping factors ($B = 0$, 1000, 3000, and 6000).

An increase of B leads to a strong decrease of ν_t at the interface for all turbulence models. However, while for the hybrid models DDES and DES this decrease of ν_t is restricted to regions close to the gas-liquid interface,

the ν_t-profiles are affected over the whole height of the channel for the k-ω and the SST model. This leads to a strong improvement of the results obtained with these models if damping is applied.

Figure 5 shows profiles of the turbulent kinetic energy, k. Again, the same turbulence models and damping factors as previously are considered. In addition, the pictures include experimental data from Fabre *et al.* [2]. For $B = 0$, the two RANS models (k-ω and SST) fail to predict the values of k correctly. Not even the shape of the k-profile is reproduced by these models. DDES and DES, on the other hand, are able to reproduce the shape of the k-profile also for $B = 0$. For DES, there is just an offset between experiment and simulation (observed in both phases). For DDES, such an offset is only observed in the lower part of the gas phase.

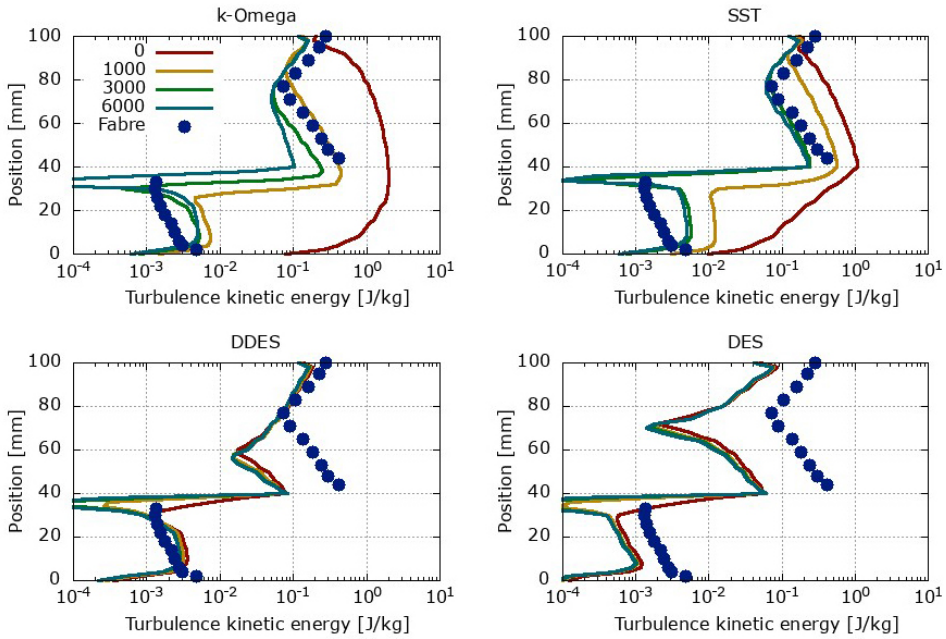

Figure 5: Profiles of the turbulent kinetic energy, k, in the centre plane at $x_3 = 9$ m (see Fig. 1) for four different turbulence models (top left – standard k-ω model, top right – $k\omega$ SST model, bottom left – hybrid SST–DDES model, bottom right – hybrid SST–DES model) and four different damping factors ($B = 0$, 1000, 3000, and 6000) in comparison with experimental data from Fabre *et al.* [2].

For $B > 0$, the RANS models are strongly improved. Regarding the gas phase, they perform even better than DDES and DES. A reason for this might be that the mesh is too coarse for the hybrid models.

3.2 Effect of damping on velocity field

Figure 6 shows the axial velocity profiles in comparison with experimental data from Fabre *et al.* [2]. One observes an enhancement of the velocity profiles for increasing damping factors for all models. However, the effect is much stronger for the two RANS models, especially for the k-ω model. Without turbulence damping ($B = 0$), the shape of the velocity profile is totally wrong compared to the experimental data. For the k-ω model, already a relatively low damping factor of $B = 1000$ leads to a significant improvement. Nevertheless, a further increase of the damping factor leads to further improvement of the velocity profiles.

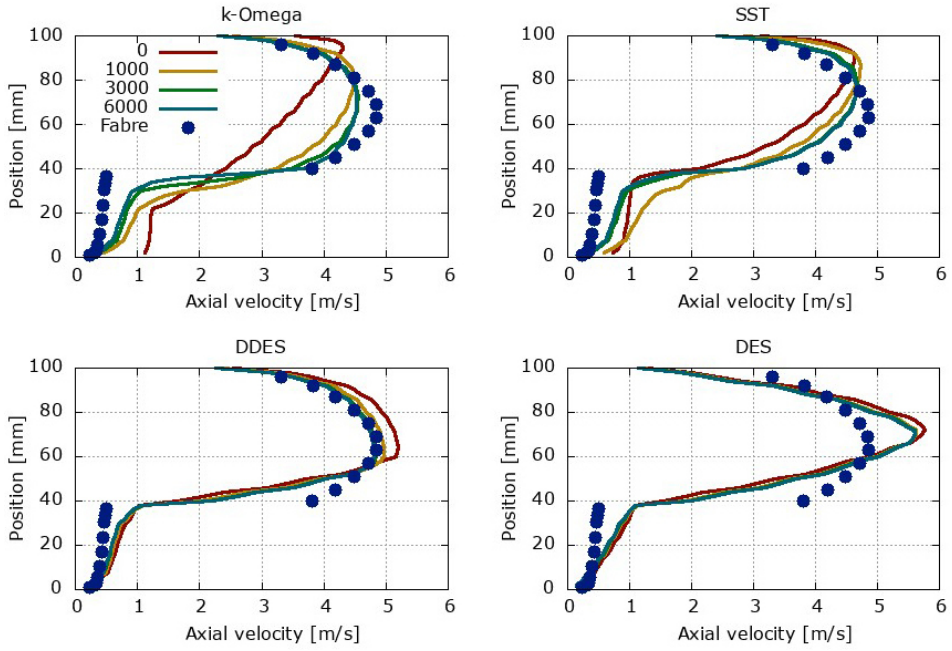

Figure 6: Profiles of axial velocity in the centre plane at $x_3 = 9$ m (see Fig. 1) for four different turbulence models (top left – standard k-ω model, top right – k-ω SST model, bottom left – hybrid SST–DDES model, bottom right – hybrid SST–DES model) and four different damping factors ($B = 0$, 1000, 3000, 6000) in comparison with experimental data from Fabre *et al.* [2].

This observation is confirmed by Fig. 7, where the mean relative error of the axial velocity on the centre plane is shown for damping factors up to $B = 20\,000$.

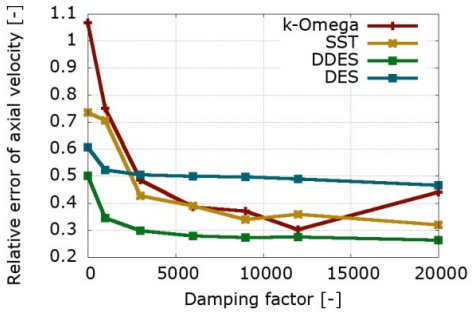

Figure 7: Mean relative error of the axial velocity in the centre plane at $x_3 = 9$ m (see Fig. 1), versus damping factor B for four different turbulence models: standard k-ω model, k-ω SST model, hybrid SST–DDES model, hybrid SST–DES model.

One observes a strong decrease of the error for the two RANS models. The two hybrid models are also enhanced by turbulence damping. However, the improvement is not as strong as for the RANS model as the error for $B = 0$ is already comparatively low.

For all turbulence models, one observes a saturation. If B is further increased, hardly any improvement can be observed. For the standard k-ω model, one recognizes even an increase of the mean relative error for $B = 20\,000$. The reason for this behaviour is that the simulation becomes unstable for too high values of B in this case. Thus, B should be chosen only as large as necessary, but not too high. In Section 3.4, the influence of the magnitude of the damping factor on the resulting pressure drop in the channel is investigated for a variety of different test cases. The results show that an appropriate value for the choice of B depends on the specific test case. Nevertheless, one can determine an appropriate value for B by means of monitoring the decrease of the pressure drop for increasing damping factors.

A comparison of the mean relative error of the DDES and the DES model shows (surprisingly) a much better performance of the (cheaper) DDES model. This observation might be explained by the fact that the resolution of the mesh is too low for a DES.

Figure 8 shows the effect of turbulence damping on the axial velocity field in a cross section at $x_3 = 9$ m.

One observes that turbulence damping does not only affect the axial velocity close to the gas-liquid interface, but also in the other parts of the channel. Especially for the k-ω model, a significant change of the velocity field in the whole cross section can be recognized.

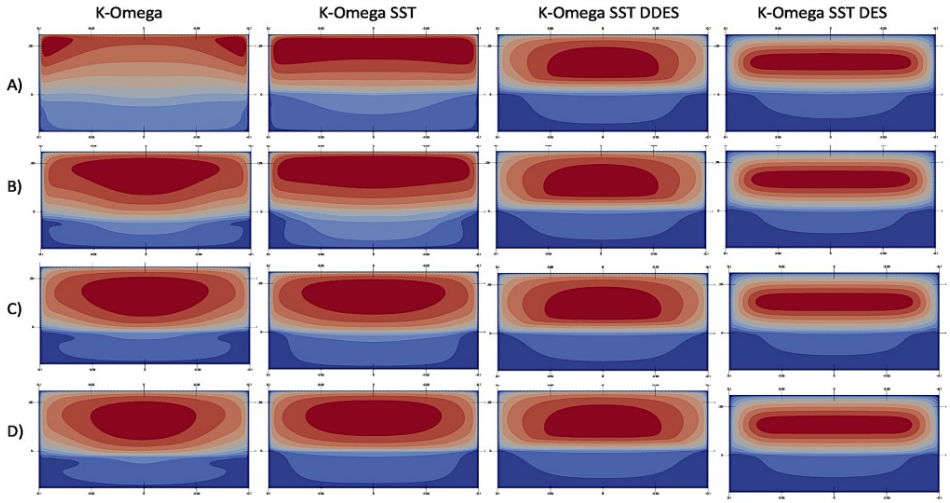

Figure 8: Axial velocity field in a cross section at $x_3 = 9$ m for four different turbulence models (from left to right: standard k-ω model, k-ω SST model, hybrid SST–DDES model, and hybrid SST–DES model) and different damping factors (from top to bottom: A) $B = 0$, B) $B = 1000$, C) $B = 3000$, D) $B = 6000$).

3.3 Influence of turbulence damping on pressure drop and height of liquid level

For both parameters, experimental data for comparison are available from Fabre *et al.* [2]. Figure 9 shows the pressure drop versus the damping factor B for the different turbulence models in comparison with experimental data [2].

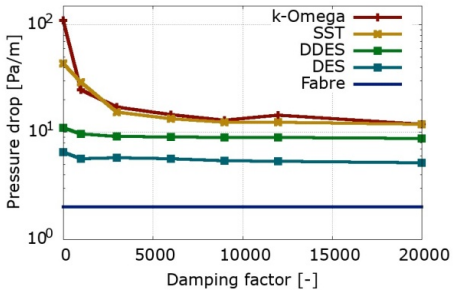

Figure 9: Pressure drop in the centre plane at $x_3 = 9$ m (see Fig. 1), versus damping factor B for four different turbulence models: standard k-ω model, k-ω SST model, hybrid SST–DDES model, hybrid SST–DES model in comparison with experimental data from Fabre *et al.* [2].

One can see how the pressure drop decreases with the increasing damping factor. This trend is observable for all turbulence models, but it is particularly dominant for the two RANS models. In this case, the pressure drop is reduced by approximately one order of magnitude. On the other hand, DDES and DES are less affected by turbulence damping in this case. Their prediction of the pressure drop is already quite good without turbulence damping (i.e. for $B = 0$).

Figure 10 shows the level of water in the centre plane at $x_3 = 9$ m for the different turbulence models in comparison with experimental data from [2].

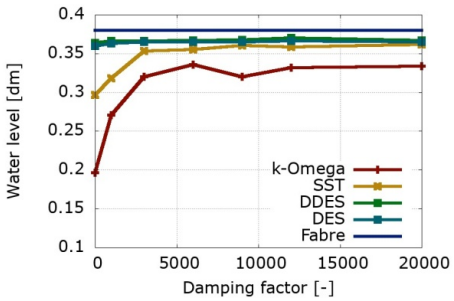

Figure 10: Level of water in the centre plane at $x_3 = 9$ m, see Fig. 1, versus damping factor B for four different turbulence models: standard k-ω model, k-ω SST model, hybrid SST–DDES model, hybrid SST–DES model in comparison with experimental data from Fabre *et al.* [2].

Similarly as for the pressure drop, one observes a strong improvement of the liquid level for the two RANS models. For the two hybrid models, the effect of damping is much lower. However, their prediction is already quite good even for $B = 0$. Altogether, the hybrid models (DDES and DES) lead to the best results. Nevertheless, a similarly good approximation of the liquid level can be obtained for the (much cheaper) SST model if a damping factor of at least $B = 3\,000$ is applied. For very high damping factors ($B = 20\,000$), hardly any difference between the SST and the hybrid models can be observed.

3.4 Influence of damping factor on pressure drop for various gas flow rates and choice of appropriate damping factor

In previous publications, different damping factors have been proposed. Egorov *et al.* [1], for example, proposed a value of $B = 100$, whereas in [26]

a value of $B = 1000$ was used. Chinello *et al.* [10] investigated the influence of different values for the damping factor for stratified air-water flows in pipes. They observed that a damping factor of $B = 250$ is sufficient for a good prediction of the pressure drop and liquid hold-up and a further increase above this value does not affect the results considerably. However, these investigations as well as comparison with our results show that different cases require different damping factors.

Hence, additional simulations for six different values of the damping factor ($B = 0, 1000, 3000, 6000, 9000, 12\,000$) and eleven different gas flow rates (15, 25, 35, 45, 55, 65, 75.4, 85, 95, 105, and 118.7 l/s) were performed using the SST model. Figure 11 shows the resulting pressure drop for the different test cases versus the magnitude of the damping factor B. For three of the eleven test cases, corresponding experimental data can be found in Fabre *et al.* [2]. These data are also plotted in Fig. 11 for comparison and validation of the simulation results.

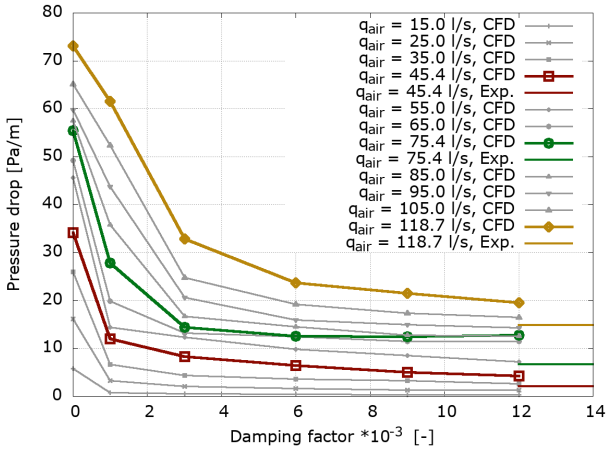

Figure 11: Calculated pressure drop using the k-ω SST model versus damping factor B for different gas flow rates (15–118.7 l/s) and a fixed liquid flow rate of 3 l/s. Comparison with experimental data from Fabre *et al.* [2] for three cases.

One observes that the higher the gas-to-liquid flow rate ratio, the higher the overprediction of the pressure drop in the channel without damping. Furthermore, in these cases, higher values of B are required to get a realistic value for the pressure drop in the channel. According to the findings in [10], it was also observed that a further increase of the damping factor did not change the resulting pressure drop anymore. However, in some of

the numerical simulations, numerical instabilities were observed for very high values of B.

In general, it can be concluded that a too high damping factor is usually not problematic as long as it does not lead to numerical instabilities in the simulation. However, since the concrete value of the turbulence damping factor can depend on the formulation of the turbulence model, it is difficult to find a value that fits all cases. Hence, for a specific application, it needs to be assured that the damping factor is not chosen too low. To avoid this problem, it is proposed to consider the resulting pressure drop for two different damping factors $B = B_1$ and $B = B_2 > B_1$ and compare it with the pressure drop for $B = 0$, which can be used as a reference. If there is still a significant decrease in the pressure drop for $B = B_2$ compared to $B = B_1$, the damping factor should further be increased. Otherwise, the damping factor is large enough and does not need to be changed. The following scheme is proposed:

1. Set $i = 1$; $B_1 = 1000$.
2. Calculate $dp(0)$, $dp(B_i)$.
3. Choose an appropriate value for $B_{i+1} > B_i$ (e.g., $B_{i+1} = (i+1)B_1$ or $B_{i+1} = 2B_i$) and calculate dpB_{i+1}).
4. Check the following condition:
   $[dpB_i) - dp(B_{i+1})]/[B_{i+1} - B_i] < \varepsilon[dp(0) - dp(B_1)]/B_1, \varepsilon = 0.1. \quad (*)$
5. If $(*)$ is fulfilled, use B_{i+1}, else increase i by one and go back to step 3.

This routine makes sure that the chosen damping factor is not too low. For the case that experimental data are available for comparison with the simulation results, such a routine is probably not needed because simulation results can directly be validated. However, in cases where no experimental data are available, such a scheme helps to justify if the predicted pressure drop of the simulation is realistic.

4 Conclusions

In this paper, the performance of turbulence damping in four different turbulence models (two RANS models, one DES model and one DDES model) was studied.

For all models, a significant increase of specific dissipation,rate close to the interface was observed. For the two RANS models, this led to a significant improvement of both the axial velocity profiles and turbulence pa-

rameters. When turbulence damping was applied, these profiles were much closer to the corresponding experimental data. Even though the source term added to the ω-equation was only active directly at the interface between the phases, it had an influence on the different parameters throughout the whole cross section. For the DDES and DES model, turbulence damping also led to an improvement of the axial velocity profile, but not as much as for the RANS models.

While the two hybrid models were able to predict the order of magnitude of the pressure drop (and hence also the height of the water level) already without turbulence damping, the two RANS models totally failed if no turbulence damping was applied. However, as soon as turbulence damping was used, the prediction of both the pressure drop and the liquid level was improved significantly.

In order to investigate the influence of the magnitude of the damping factor on the pressure drop predicted by the numerical simulations, a variety of different test cases were considered. The results showed that the higher the gas-to-liquid flow rate ratio, the higher the overprediction of the pressure drop in the channel without damping. Furthermore, in these cases, higher values of model parameter, B, are required to get a realistic value for the pressure drop in the channel. Finally, a scheme for the determination of an appropriate value for the model parameter was proposed.

Acknowledgement This work was supported through the Joint Research Project Multiphase flow reference metrology. This project has received funding from the EMPIR programme co-financed by the Participating States and from the European Union's Horizon 2020 research and innovation programme. The authors would like to thank Marc Olbrich from Physikalisch-Technische Bundesanstalt (PTB) and Stanislav Knotek from Czech Metrology Institute (CMI) for fruitful discussions.

Received 1 June 2021

References

[1] Egorov Y., Boucker M., Martin A., Pigny S., Scheuerer M., Willemsen S.: *Validation of CFD codes with PTS-relevant test cases*. Tech. Rep. EVOL-ECORA-D07, 2004.

[2] Fabre J., Masbernat L., Suzanne C.: *Stratified flow. Part I: Local structure*. Multiphas. Sci. Technol. **3**(1987), 285–301.

[3] Höhne T., Vallée C.: *Experiments and numerical simulations of horizontal two-phase flow regimes using an interfacial area density model*. J. Comput. Multiphas. Flow. **2**(2010), 3, 131–143.

[4] Vallée C., Höhne T.: *CFD validation of stratified two-phase flows in a horizontal channel*. In: Annual Report 2006 (F.-P. Weiss, U. Rindelhardt, Eds.), FZR-465, Forschungszentrum Dresden Rossendorf, 2007, 33–38.

[5] Frederix E.M.A., Mathur A., Dovizio D., Geurts B.J., Komen E.M.J.: *Reynolds-averaged modeling of turbulence damping near a large-scale interface in two-phase flow*. Nucl. Eng. Design **333**(2018), 122–130.

[6] Höhne T., Vallée C.: *Modelling of stratified two phase flows using an interfacial area density model*. In: Proc. Multiphase Flow 2009, 5th Int. Conf. on Computational and Experimental Methods in Multiphase and Complex Flow, New Forest, 15-17 June, 2009, 123–133.

[7] Höhne T., Mehlhoop J.-P.: *Validation of closure models for interfacial drag and turbulence in numerical simulations of horizontal stratified gas–liquid flows*. Int. J. Multiphas. Flow **62**(2014), 1–16.

[8] Porombka P., Höhne,T.: *Drag and turbulence modelling for free surface flows within the two-fluid Euler–Euler framework*. Chem. Eng. Sci. **134**(2015), 348–359.

[9] *Ansys Fluent User's Guide. Release 2021 R1*. Ansys, Inc., Canonsburg 2021.

[10] Chinello G., Ayati A.A., McGlinchey D., Ooms G., Henkes R.: *Comparison of computational fluid dynamics simulations and experiments for stratified air-water flows in pipes*. J. Fluid. Eng. **141**(2019), 5, 051302-1– 051302-12.

[11] Gada V.H., Tandon M.P., Elias J., Vikulov R., Lo S.: *A large scale interface multi-fluid model for simulating multiphase flows*. Appl. Math. Model. **44**(2017), 189–204.

[12] Lo S., Tomasello A.: *Recent progress in CFD modelling of multiphase flow in horizontal and near-horizontal pipes*. In: Proc. 7th North American Conf. on Multiphase Technology, Banff, June 2010, BHR-2010-F1.

[13] Fan W., Li H., Anglart H.: *Numerical investigation of spatial and temporal structure of annular flow with disturbance waves*. Int. J. Multiphas. Flow **110**(2019), 256–272.

[14] Fan W., Anglart H.: *Progress in phenomenological modeling of turbulence damping around a two-phase interface*. Fluids **4**(2019), 3, 136.

[15] Fan W., Anglart H.: *varRhoTurbVOF 2: Modified OpenFOAM volume of fluid solvers with advanced turbulence modeling capability*. Comput. Phys. Commun. **256**(2020), 107467.

[16] Wilcox D.C.: *Turbulence Modeling for CFD* Vol. 2. DCW Industries, La Canada 1998.

[17] Menter F., Kuntz M., Langtry R.: *Ten years of industrial experience with the SST turbulence model*. In: Turbulence, Heat and Mass Transfer 4 (K. Hanjalic, Y. Nagano, M. Tummers, Eds.). Begell House, 2003.

[18] Langtry R.B., Menter F.R.: *Correlation-based transition modeling for unstructured parallelized computational fluid dynamics codes*. AIAA J. **47**(2009), 12, 2894–2906.

[19] Egorov Y., Menter F.: *Development and application of SST-SAS turbulence model in the desider project*. In: Advances in Hybrid RANS-LES Modelling (S.-H. Peng, W. Haase, Eds.), Springer, Berlin Heidelberg, 2008, 261–270.

[20] Strelets M.: *Detached eddy simulation of massively separated flows*. In: Proc. 39th AIAA Aerospace Sciences Meet. Exhib., Reno, Jan. 8-11, 2001.

[21] Gritskevich M., Garbaruk A., Schütze J., Menter F.: *Development of DDES and IDDES formulations for the k-ω shear stress transport model*. Flow Turbul. Combust. **88**(2012), 3, 431–449.

[22] Müller-Steinhagen H., Heck K.: *A simple friction pressure drop correlation for two-phase flow in pipes*. Chem. Eng. Process. **20**(1986), 6, 297–308.

[23] Launder B., Spalding D.: *The numerical computation of turbulent flows*. Comput. Methods Appl. Mech. Eng. **3**(1974), 2, 269– 289.

[24] Menter F.R.: *Two-equation eddy-viscosity turbulence models for engineering applications*. AIAA J. **32**(1994), 8, 1598–1605.

[25] Spalart P., Deck S., Shur M., Squires K., Strelets M., Travin A.: *A new version of detached-eddy simulation, resistant to ambiguous grid densities*. Theor. Comput. Fluid Dyn. **20**(2006), 181–195.

[26] Frank T.: *Numerical simulation of slug flow regime for an air-water two-phase flow in horizontal pipes*. In: Proc. 11th Int. Topical Meeting on Nuclear Reactor Thermal-Hydraulics (NURETH-11), Avignon, Oct. 2–6, 2005.